JOURNAL OF SPACECRAFT AND ROCKETS
Vol. 41, No. 2, March–April 2004

Development of Protective Coatings for High-Temperature Metallic Materials

R. Keith Bird* and Terryl A. Wallace*
NASA Langley Research Center, Hampton, Virginia 23681
and
Sankara N. Sankaran†
Lockheed Martin Space Operations, Hampton, Virginia 23681

Metallic material systems with potential for high-temperature operations are critical for many land-based and space-based systems. Advanced alloys with improved elevated temperature properties and/or reduced densities offer improved structural efficiency and longer service life compared to more conventional alloys. However, in extreme operating environments, these alloys require coatings for environmental protection and thermal control. We discuss some results from a program to develop ultrathin, lightweight, protective coatings applied via sol-gel techniques for some emerging high-temperature alloys. The coatings were designed to reduce oxidation, increase emittance, and reduce the catalytic efficiency for recombination of dissociated hot-gas species for the candidate materials. The alloys considered in this study include PM1000 (an oxide dispersion strengthened Ni-based alloy), 602CA Ni-based alloy, and a gamma titanium aluminide alloy. Inconel 617, a Ni-based alloy, was included as a reference. Microstructural analysis and oxidation weight gain results indicated that the coatings significantly reduced oxidation damage during extended high-temperature exposures for these alloys. In addition, one coating system was shown to improve the emittance of Inconel 617. A substantial reduction in the recombination of atomic nitrogen and oxygen at the surface of Inconel 617 substrates in a hot flowing airstream was also observed.

Introduction

DEVELOPMENT of temperature-resistant metallic materials is an enabling technology for many high-temperature structural applications. Examples of such applications include hot structures and thermal protection systems for hypersonic flight vehicles that reenter the Earth's atmosphere under extreme temperature and environmental conditions. For these types of applications, thin-gauge metallic sheet and foil are typically used, where possible, to minimize structural weight. However, these thin-gauge materials can be susceptible to environmental damage because a significant fraction of the material cross section can be affected by the environment. Thus, protective coatings may be required to prevent degradation of thin-gauge metal structures in severe, high-temperature service conditions. The coatings can also be used to modify the surface of the structure to enhance its thermal control characteristics. For many applications, a high emittance is desirable to reduce significantly the amount of heat that is absorbed by the structure. Also, in hot flowing air environments, where gaseous species (such as oxygen and nitrogen) have been dissociated into their atomic form, the recombination of these atoms into their molecular form at the surface can cause significant increases in heat input to the structure. Catalytic efficiency, or recombination efficiency, is a measure of the propensity of a material to promote this recombination and can vary significantly for different materials. For metallic materials, the catalytic efficiency is relatively high, and coatings that reduce the efficiency of this recombination reaction can greatly reduce the structural temperature.

This paper discusses work at NASA Langley Research Center (LaRC) to develop ultrathin (<5-μm), lightweight, sol-gel-based coatings that offer environmental protection and thermal control for several alloys that are candidates for high-temperature applications. Two relatively new nickel-based superalloys, PM1000 and 602CA, were evaluated for applications in the 1000–1100°C upper temperature range. Inconel 617, which is a state-of-the-art conventional nickel-based superalloy, was used as a baseline for comparison. In addition, a low-density gamma TiAl intermetallic alloy was evaluated for applications with an upper use temperature of 870°C. Oxidation performance of the alloys and coatings was determined in both a static air environment and in a hot flowing airstream. Room temperature emittance was measured before and after static air exposure and catalytic efficiency was measured in the hot airstream. In addition, tensile properties of uncoated alloy sheet specimens were determined before and after oxidation exposures.

Materials

Table 1 shows the nominal composition and density of the alloys used for this study. All of the materials were in the form of sheets. Inconel 617 is a state-of-the-art nickel-based superalloy with good strength and creep resistance for high-temperature applications.[1] It was used as a baseline with which to compare the performance of the other alloys. A cold-rolled and annealed sheet with a thickness of 0.15 mm was used in this study. Alloy 602CA is a recently developed nickel-based superalloy[2] with reported mechanical properties and oxidation behavior similar to Inconel 617. In addition, 602CA is readily cold rollable to thin sheets and foils, which makes it amenable to incorporation into lightweight thin-gauge structures. Alloy 602CA also has a density that is approximately 6% less than that of Inconel 617, making it attractive for high-temperature aerospace structures where weight is critical. Cold-rolled and annealed 602CA sheets with thicknesses of 0.05 and 0.08 mm were evaluated. PM1000 is a mechanically alloyed nickel-based superalloy[3] with a fine dispersion of Y_2O_3 particles for increased high-temperature strength and corrosion resistance at temperatures on the order of 1100°C. The density of PM1000 is slightly lower than that of Inconel 617. The PM1000 sheet evaluated in this study had a thickness of 0.25 mm. The titanium aluminide alloy investigated in this study was based on gamma TiAl with alloy additions to increase room temperature ductility.[4] This alloy has a density that is less than one-half that of the nickel alloys. Because of difficulties in producing very thin gauges of this alloy, a sheet with a thickness of 1 mm was used.

Received 13 June 2002; revision received 21 October 2002; accepted for publication 4 November 2002.

*Materials Research Engineer, Metals and Thermal Structures Branch.
†Senior Scientist and Metals Group Leader, Langley Program Office.

Table 1 Composition and density of alloys evaluated for high-temperature applications

Alloy	Composition, wt%										Density, g/cm^3
	Ni	Cr	Fe	Co	Mo	Al	Ti	Nb	Ta	Other	
Inconel 617 (Ref. 1)	——[a]	22	1.5	12.5	9	1.2	——	——	——		8.4
602CA (Ref. 2)	——[a]	25	9.5	——	——	2.1	0.15	——	——	0.1 Y, 0.05 Zr, 0.2 C	7.9
PM1000 (Ref. 3)	——[a]	20	3	——	——	0.3	0.5	——	——	0.6 Y_2O_3	8.2
Gamma TiAl (Ref. 4)	——	3.2	——	——	——	32	——[a]	2.4	2.4	0.03 B	3.7

[a]Remaining balance of composition.

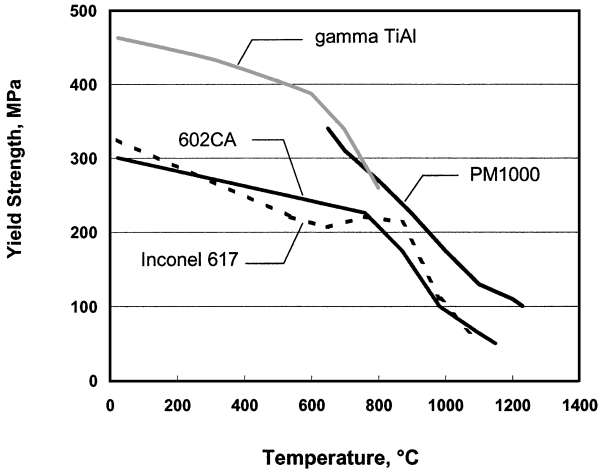

Fig. 1 Yield strength of Inconel 617 (Ref. 1), 602CA (Ref. 2), PM1000 (Ref. 3), and gamma TiAl (Ref. 4).

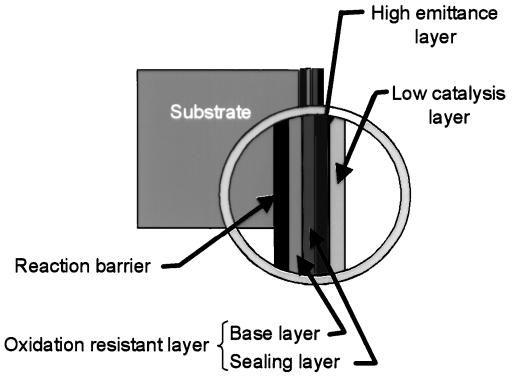

Fig. 2 Schematic diagram of the coating concept.

Figure 1 shows the yield strengths of Inconel 617, PM1000, 602CA, and gamma TiAl as functions of temperature. The data show that the yield strength behavior of 602CA is similar to that of Inconel 617, and that all three Ni-based alloys have useful yield strength at temperatures to about 1100°C. Gamma TiAl exhibits high yield strength at the lower temperatures but begins rapidly losing strength in the 800°C regime and is potentially usable to about 870°C.

Coatings

The sol-gel process was selected for coating development because of its simplicity of application; its ability to produce very thin, lightweight coatings; and its potential for ease of scaleup and field repair. Sol-gels are colloidal aggregates produced by destabilizing and drying metal–hydroxide and metal–salt solutions. When heated, they decompose into oxides, densify, and, at sufficiently high temperatures, crystallize. Decomposition temperatures are generally below 500°C, and full densification temperatures are generally below 1000°C. The sol-gel process is an effective route for the fabrication of ceramic oxide coatings. Sol-gels have major advantages for practical application: a) relatively low processing temperatures, b) potential for coating large and complex areas, and c) good homogeneity and high purity. In principle, it should be possible to prepare an oxide coating of almost any composition from sol-gels, provided that the appropriate starting materials are chosen.

In the sol-gel process, a precursor coating is formed from a metal–organic solution that is applied as a liquid at room temperature. The next step in the process is the gel formation that will occur at room temperature but that can be accelerated by heating. The final step is curing, in which the precursors decompose into oxides and densify. Detailed discussions of sol-gel chemistry and processing can be found in Refs. 5 and 6.

A variety of methods like dipping, brushing, or spraying can be used to apply precursor sol-gel coatings to the substrate. For uniform thin coatings, dip coating produces good results. The setup for applying sol-gel coatings is typically simple and inexpensive and primarily consists of a container to hold the sol and a mechanism to dip and withdraw the coated part at a specific rate. The drying of the sol is preferred in a dry nitrogen environment to avoid moisture pickup by some of the organic precursors. Gel formation begins at room temperature and is accelerated through heating. For industrial applications, heating jackets for drying and heaters for curing can be incorporated into the design. The coating thickness, uniformity, and integrity are controlled by the sol chemistry, viscosity of the sol, and by the rate of withdrawal of the specimen from the sol. Once the coating is cured, it is environmentally inert and stable.

A multilayered coating design has been adopted for meeting the oxidation, emittance, and low catalysis characteristics needed in hypersonic structures. This coating design consists of up to five types of layers and is shown schematically in Fig. 2. The outermost layer is designed for low catalytic efficiency to minimize aerothermodynamic heating and is based on borosilicate or borophosphate glasses. The high-emittance layer consists of various constituents, such as SiB_6, that provide emittance enhancement to the total system. It is shown as the second layer from the outer surface, but its location may be changed to optimize the combination of oxidation resistance and emittance. The oxygen-resistant layer is an oxygen diffusion barrier comprised of a two-phase glass. This two-phase glass layer has a predominantly SiO_2 matrix phase and a discontinuous second phase, with a lower glass transition temperature that can flow and facilitate self-healing behavior. In some cases, this layer was constructed with two sublayers: the base and an outer sealant that is similar in content to the base but with a higher proportion of the phase with the lower glass transition temperature to promote fluidity and sealing effectiveness in the coating. A reaction barrier layer is required in most alloys to prevent reaction between the substrate alloy and the other coating layers. This layer typically consisted of a sol-gel-based Al_2O_3 layer, although $TiAl_3$ was also considered as an alternative reaction barrier for gamma TiAl. It is recognized that thermal expansion coefficient differences between layers are inherent in this multilayer design. However, the thin nature of the coating helps to accommodate thermal strains, and the self-healing characteristics help to overcome the consequences of cracking that may occur.

The compositions of the individual layers differ for alloys of different classes. In addition, current results indicate that the coatings may need to be tailored for specific alloys within the same class, but with different chemistries, such as Inconel 617 and PM1000 Ni-based superalloys. The development strategy and the coating design are described in more detail in Ref. 7.

Experimental Procedures

Coating

Before application of the various coating layers, the specimens were cleaned in detergent, rinsed with acetone followed by

methanol, and blotted dry. In the case of gamma TiAl, the specimens were further cleaned in a solution of hydrofluoric acid, nitric acid, and water to remove residual oxides from the surface. The individual coating layers were applied to the test specimens using the sol-gel dipping technique described in the preceding section. After the application of each layer, the specimens were heated to the curing temperature of 650°C for 5 min. The innermost layers of the coating comprised a ~2-μm-thick reaction barrier and a ~2-μm-thick glass diffusion barrier with a sealant. Sol-gel-based Al_2O_3 was applied as the reaction barrier. In addition, $TiAl_3$ was investigated as an alternate reaction barrier for gamma TiAl because it has been found to be a good reaction barrier on other titanium alloys.[7–9] The $TiAl_3$ was formed by depositing a 1-μm-thick layer of aluminum by electron beam vapor deposition, followed by vacuum annealing at 620°C for 8 h.

The catalysis layer is required to be the outermost layer and was, therefore, applied on the top of the other layers using the sol-gel process. Emittance layers were originally conceived of as an intermediate layer between the oxidation and catalysis layers and were, therefore, applied on top of the oxidation layers. Because the emittance and catalysis layers were isolated from the alloy surface by the oxidation protection layers, their performance was considered to be independent of the alloy on which they were applied. Accordingly, development and testing of these layers were limited to the Inconel 617 alloy.

Oxidation Exposures

Rectangular coupon specimens of various sizes were used for the oxidation exposure studies. In each case, the dimensions of the coupons were measured, and the surface area was computed to normalize the weight-gain data. Isothermal oxidation of the samples was conducted in a horizontal tube furnace or in a muffle furnace in laboratory air, with the temperature maintained to within ±3°C. These exposures were not strictly isothermal because the tests were interrupted periodically to monitor the weight gained/lost by the specimens. After the furnace was shut off and the samples were allowed to cool in the furnace, the samples were removed and weights measured to an accuracy of ±0.01 mg. Isothermal tests were continued for a cumulative exposure up to 100 h. Both coated and uncoated specimens were subject to the oxidation exposure studies. This technique was used for oxidation studies so that all of the coated and uncoated specimens could be exposed simultaneously to the same environment and temperature. Also, the interrupted exposure imposed a greater severity on the coating due to thermal cycling. However, the advantages of a thermogravimetric analysis in terms of mechanistic details were not obtained.

The exposure temperature used for the oxidation studies varied depending on the intended use temperature of the alloys. The Inconel 617 specimens were evaluated at 1000°C, whereas PM1000 specimens were evaluated at 1100°C. The 602CA specimens were evaluated at both 1000 and 1100°C. The gamma TiAl specimens were evaluated only at 870°C. In addition, uncoated Inconel 617 and 602CA tensile specimens were exposed to oxidation environments at 980°C for up to 100 h. Weight gain was periodically monitored and postexposure tensile properties were measured at room temperature.

Metallurgical Analysis

Metallography was performed on the surfaces and mounted cross sections of selected specimens after the oxidation exposure. These studies were performed on both coated and uncoated specimens. Scanning electron microscopy was used as the main technique for metallography, using a JEOL JSM 6400 scanning electron microscope (SEM). Energy dispersive spectroscopy was used to perform elemental analysis and distribution maps in both coated and uncoated specimens using an EDAX EDAM 3 unit attached to the SEM. All of the data were stored in digital format. For cross-sectional examination, the specimens were in the unetched condition.

Tensile Tests

Room temperature tensile properties of Inconel 617 and 602CA were measured before and after oxidation exposures in accordance with American Society for Testing and Materials designation E8 (Ref. 10). Subsize tensile specimens with a test-section width of 6.4 mm were machined from the alloy sheets. Tests were conducted in a closed-loop hydraulic test system with hydraulic grips. Strain was monitored with back-to-back extensometers with 1-in. gauge length. Specimens were loaded at a stroke rate of 0.25 mm/min until 2% total strain was attained, at which point the stroke rate was increased to 1.25 mm/min.

Emittance Tests

The room-temperature emittance of coated and uncoated coupons was determined before and after oxidation exposure. Room-temperature total reflectance measurements were made using a Gier Dunkle DB100 reflectometer. Total emittance was then calculated using the relationships that absorptance equals unity minus reflectance and (from Kirchhoff's law) that emittance equals absorptance under steady-state conditions.

Hypersonic Environmental Tests

Candidate coatings and materials were exposed to simulated hypersonic flow environments in the NASA LaRC Hypersonic Materials Environmental Test System (HYMETS). This test facility is a 100-kW constricted-arc heated wind tunnel that consists of the arc heater and a test chamber with four model insertion stings. Samples measuring 25 mm in diameter were mounted in a stagnation configuration on two of the insertion stings. The other stings contained a water-cooled heating rate probe and a pressure probe that measured the cold-wall heating rate and surface pressure, respectively. The test gas was a mixture of air plus nitrogen and oxygen in ratios equivalent to air. High-purity nitrogen was introduced at the cathode, and air and high-purity oxygen were introduced upstream of the supersonic nozzle. The facility can produce airflow up to about Mach 5. The temperature of the samples during exposure was monitored by a thermocouple attached to the back surface of the sample. Chemical equilibrium calculations have indicated that oxygen in the test stream was almost fully dissociated (>95%), whereas the nitrogen was only slightly dissociated (<5%) (Ref. 11).

HYMETS exposures were conducted in 30-min increments, during which each sample temperature was maintained at 980 ± 3°C by adjusting the power input to the test facility. For each test, the operating conditions of the HYMETS and the fully catalytic heating rate (measured by a silver slug calorimeter) were recorded. Samples were periodically removed from the HYMETS and weight change was measured using an analytic balance. Total emittance at the test temperature was calculated before and after exposure from room-temperature near-normal spectral reflectance data collected over the wavelength from 1.5 to 25 μm using a Gier Dunkle Model HCDR 3 heated cavity reflectometer.

The catalytic efficiency was calculated from an energy balance at the specimen surface using a technique developed by Clark et al.[12] First, the fully catalytic heating rate was calculated using Goulard's solution to determine the enthalpy of the test environment, then the calculated heating rate was used with Goulard's solution to determine the catalytic efficiency of the specimen surface. Because this technique depends on empirical adjustments to theoretical equations, the results can be quite sensitive to uncertainties in experimental parameters, and the maximum uncertainty can be as high as 45% for materials with low catalytic efficiencies. The results, therefore, must be considered nominal and are used primarily for screening and the development of candidate coatings.

Results and Discussion

Oxidation Behavior of Superalloys

Figure 3 shows the tensile ductility, as measured by plastic strain to failure, of 0.05- and 0.08-mm-thick 602CA sheets and a 0.15-mm-thick Inconel 617 sheet as a function of oxidation weight gain after exposure at 980°C. The sheets showed a consistent decrease of ductility with increased weight gain, with the ductility of the 0.05-mm 602CA sheet approaching zero at about 0.7 mg/cm^2 weight gain. If a nominal 10% strain to failure is desirable for structural applications, oxidation weight gain should be kept to less than about 0.4 mg/cm^2 for the 0.05-mm 602CA sheet and about

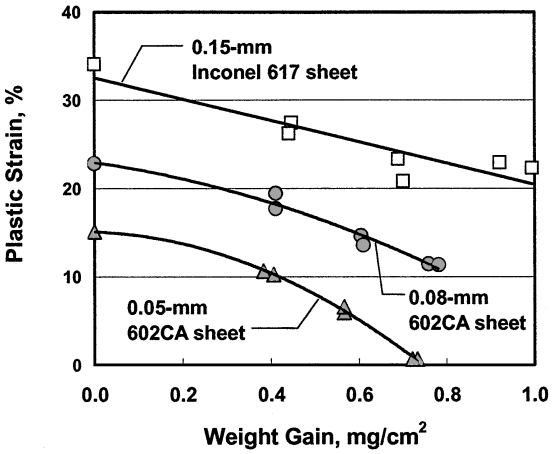

Fig. 3 Room temperature ductility of uncoated superalloy sheet exposed in air at 980°C.

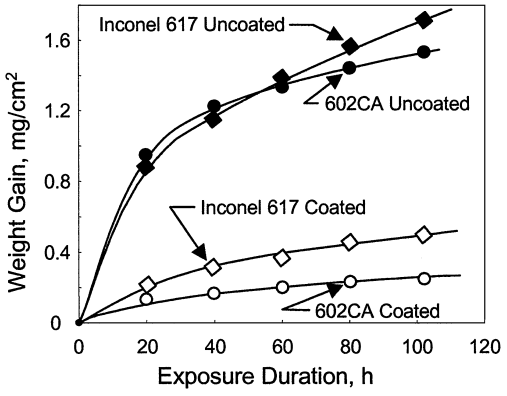

Fig. 4 Oxidation performance of Inconel 617 and 602CA at 1000°C in air.

0.7 mg/cm^2 for the 0.08-mm 602CA sheet. Figure 3 also shows that the ductility is consistently higher for the thicker sheets. The 0.15-mm Inconel 617 sheet maintained a ductility exceeding 20% for all exposures because it started with a ductility (35%) much higher than that of the thinner 602CA sheets. However, after a 100-h exposure, corresponding to approximately 1-mg/cm^2 weight gain, the Inconel 617 sheet ductility had been reduced to 60% of its unexposed value, indicative of significant oxidation damage.

The oxidation behavior of the alloys was evaluated using weight-gain data as a function of exposure duration. A potential uncertainty in the weight-gain measurement can be caused by spallation of the coating and/or reaction products during specimen handling. However, spallation usually results in drastic specimen weight loss to an extent that it can be easily identified. Figure 4 shows the weight-gain data at 1000°C for both Inconel 617 and 602CA alloys in the coated and uncoated conditions. The weight-gain values measured for uncoated Inconel 617 were about 30% greater than those reported by Christ et al.,[13] who used thermogravimetric analysis to measure the oxidation rates in this alloy. It is not clear whether handling during the interrupted oxidation measurement in the present study has contributed to this difference. The oxidation behaviors of uncoated Inconel 617 and 602CA alloys are similar at 1000°C. The coated specimens show 5–10 times lower weight gain compared to the corresponding uncoated alloy after exposure for 100 h, but the coating appears to be more effective on 602CA. Figure 5 shows weight-gain data at 1100°C for alloys PM1000 and 602CA. This alloy shows better oxidation performance compared to the 602CA alloy in the uncoated condition. The coated PM1000 alloy specimens also performed better than the coated 602CA; however, both coatings produced weight gains that were 4–5 times lower than the corresponding uncoated alloy.

Cross-sectional SEM images of uncoated specimens are shown in Fig. 6. The elemental maps of the predominant species for the

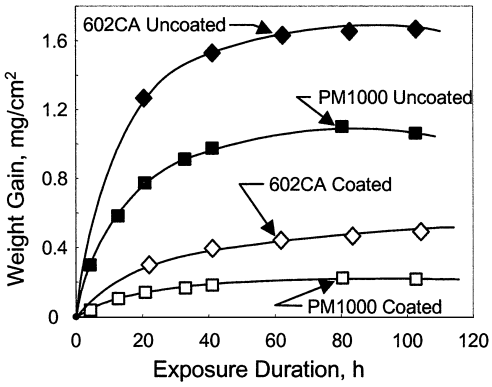

Fig. 5 Oxidation performance of 602CA and PM1000 at 1100°C in air.

specimens in the uncoated condition after oxidation exposure are presented in Fig. 7. All three alloys form a Cr_2O_3 layer as the oxidation product on the surface of the specimens, consistent with the results reported in the literature[13–15] for the oxidation behavior of Ni/Cr alloys with chromium content >10%. Also, at temperatures above 900°C, Cr_2O_3 oxidizes further to CrO_3, which is volatile.[14] Volatility of Cr_2O_3 explains the decrease in rate of weight gain at a longer exposure duration noted in Figs. 4 and 5.

The Inconel 617 and 602CA alloys also display an oxidation product along the grain boundaries. This internal oxidation phenomena was observed in the 602CA alloy after exposure at both temperatures: the depth of the internal oxidation layer was ~10 μm after the 1000°C exposure and ~25 μm after the 1100°C exposure. The elemental maps indicate that the internal oxide was probably Al_2O_3. The chemical composition of Inconel 617 and 602CA fall within the range of Group II alloys defined by Giggins and Pettit.[16] In Group II alloys, aluminum transport is slow and aluminum is precipitated as an internal oxide, whereas chromium diffusion is fast enough to promote a continuous Cr_2O_3 outer layer. The results on Inconel 617 and 602CA alloys conform to this behavior. The Inconel 617 microstructural observations also agree with the observations of Christ et al.[13] However, on 602CA, Brill and Agarwal[17] have reported formation of a protective Al_2O_3 layer on the surface of the alloy below the Cr_2O_3 layer (no internal oxidation) when 602CA was tested in air at 1200°C. This difference suggests that the diffusivity of aluminum in the alloy at 1200°C may be sufficient to form continuous Al_2O_3 but may not be adequate at 1000 and 1100°C to avoid internal oxidation.

The Al map has not been displayed for the PM1000 alloy because it does not show any grain boundary oxidation, but the metal/oxide interface shows a high degree of roughness. Unevenness develops at the metal/oxide interface during the oxidation of alloys in which one of the minority elements form the oxidation product. This roughening is caused by the growth of any initial inward protuberance due to shortening of diffusion distances in the region that eventually develops into a wavy interface.[18] PM1000 alloy is also characterized by substantial Kirkendall porosity that substantiates this phenomenon. The elemental maps show that nickel did not appear to participate in the oxide formation process in any of the alloys studied, even though it is the predominant constituent in these alloys. The mixed oxides of $Cr_2O_3 + NiO + NiCr_2O_4$, noted by Weinbruch et al.[19] on PM1000 exposed to air at 1100°C for durations exceeding 10 h, were not observed.

The cross-sectional micrographs of the coated specimens of Inconel 617, 602CA, and PM1000 alloys are shown in Fig. 8. Given that the coatings themselves constitute a thickness of ~4 μm, the outer layers do not seem to indicate any oxide formation. PM1000 also shows a very smooth coating/alloy interface, confirming the oxidation protection offered by the coating. Inconel 617 alloy, on the other hand, does show some internal oxidation along the grain boundaries just below the coating/alloy interface, indicating that the coating was not completely effective in stopping this process. Most regions of coated 602CA show excellent performance of the coating with neither oxide formation nor internal grain boundary oxidation.

The x-ray maps confirm the features observed in the cross-sectional micrographs. Figure 9 provides an example of typical x-ray

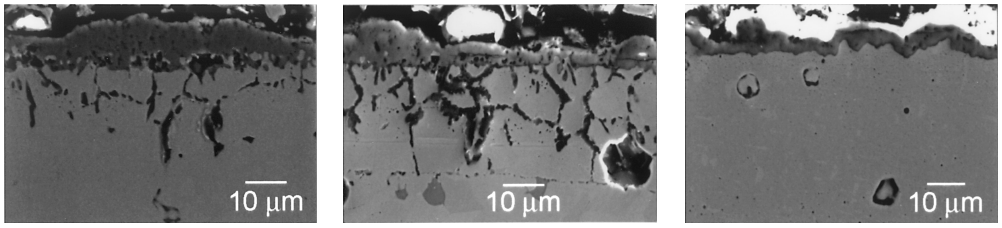

a) b) c)

Fig. 6 Cross-sectional micrographs of the uncoated specimens after oxidation: a) Inconel-617 after oxidation exposure at 1000°C for 100 h, b) 602CA after oxidation exposure at 1100°C for 100 h, and c) PM1000 after oxidation exposure at 1100°C for 100 h.

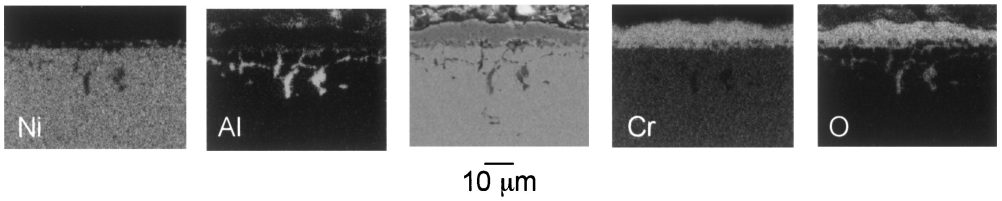

Inconel-617 after oxidation exposure at 1000°C for 100 h

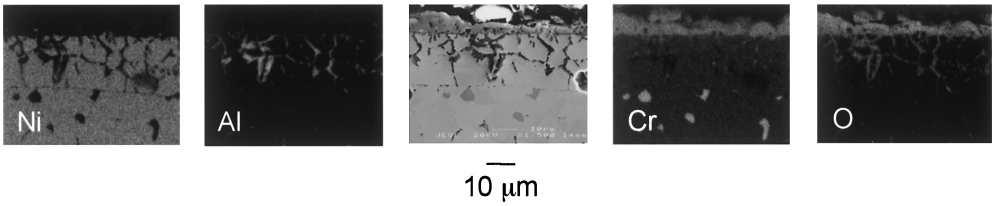

602CA after oxidation exposure at 1100°C for 100 h

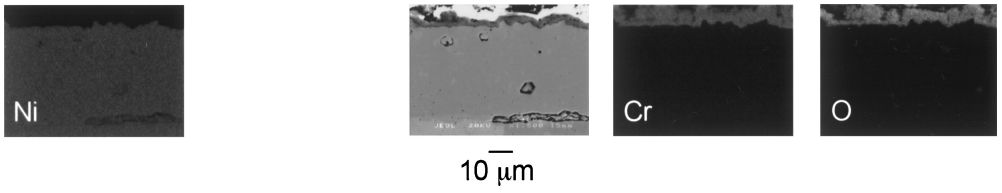

PM1000 after oxidation exposure at 1100°C for 100 h

Fig. 7 Cross-sectional micrographs and elemental x-ray maps of uncoated superalloys after oxidation.

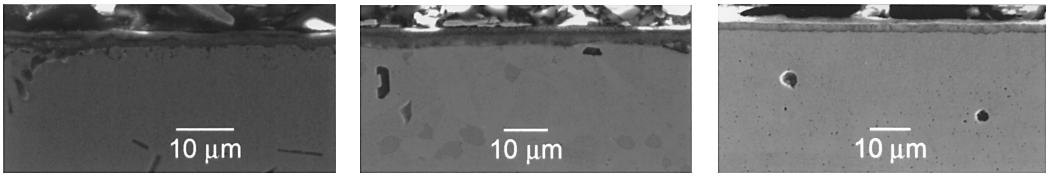

a) b) c)

Fig. 8 Cross-sectional micrographs of the coated specimens after oxidation: a) coated Inconel 617 after exposure at 1000°C for 100 h, b) coated 602CA after exposure at 1100°C for 100 h, and c) coated PM1000 after exposure at 1100°C for 100 h.

maps obtained on coated specimens. In this example, the maps are shown for coated 602CA alloy after oxidation at 1100°C for 100 h. The maps of aluminum, silicon, and oxygen, which are components of the coating, confirm that the coating remained intact even after the oxidation exposure. Furthermore, the chromium map shows no indication of chromium diffusion from the alloy into the coating and, thus, no subsequent Cr_2O_3 formation.

Because all of the superalloys were coated with the same types of coating and utilized the same coating thickness, the oxygen permeation rates through the coatings were expected to be similar for a given temperature. Based on this argument, one would expect similar oxygen weight-gain rates for all of the alloys when exposed to the same oxidation temperature. The oxidation weight-gain data shown in Figs. 4 and 5 show that the performance of the coatings varied from alloy to alloy. In fact, Inconel 617 showed the highest weight gain after 100 h exposure at 1000°C, even when compared with the weight-gain data for 602CA and PM1000 materials after exposure for the same duration at a much higher temperature (1100°C). These differences in oxidation behavior become apparent when subtle differences in the cross-sectional micrographs and elemental distribution are noted (Fig. 10). In Fig. 10, high-magnification micrographs and elemental x-ray maps of the coated and exposed specimens of all three superalloys (Inconel 617, 602CA, and PM1000) are compared. Among the three alloys, PM1000 displayed the cleanest interface between the coating and the alloy. However, comparing the aluminum and chromium maps with the micrograph shows that Cr_2O_3 formed under the coating. This can be rationalized from the permeation of oxygen through the coating at 1100°C potentially being sufficiently high to form the oxide under the coating. Alternatively, the diffused chromium map for the coated PM1000 suggests that the Al_2O_3 may not be effective as a reaction barrier. However, because the coated PM1000 exhibited low weight gain, the thin silica layer appears to offer substantial oxidation protection. In the case of 602CA, comparison of the micrograph with the chromium map shows that chromium was predominantly confined within the alloy and did not enter the coating. However, some regions of the alloy

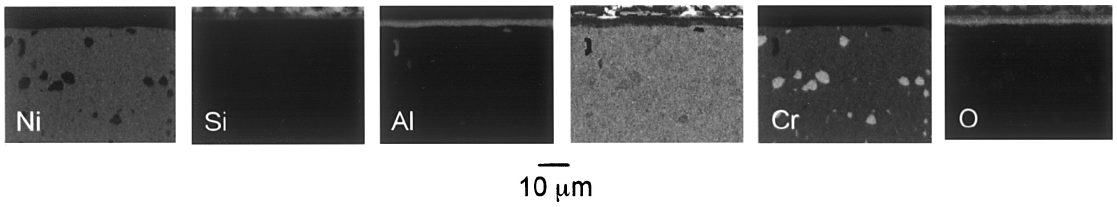

Fig. 9 Cross-sectional micrographs and elemental x-ray maps of coated 602CA after oxidation exposure at 1100°C for 100 h.

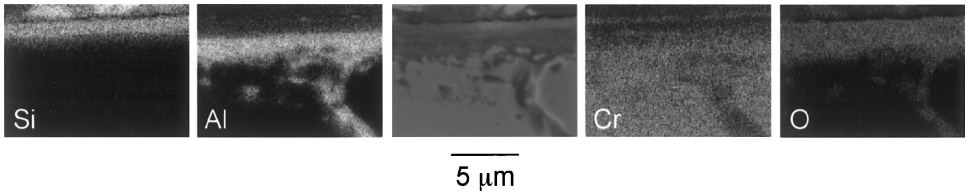

Coated Inconel 617 after oxidation exposure at 1000°C for 100 h

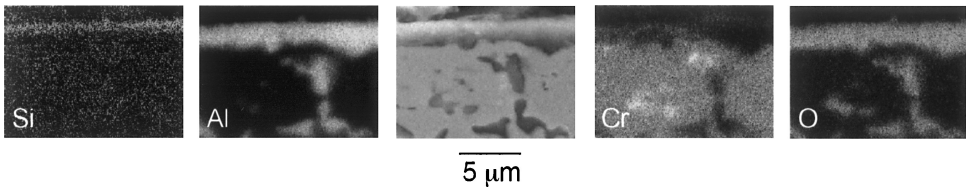

Coated 602CA after oxidation exposure at 1100°C for 100 h

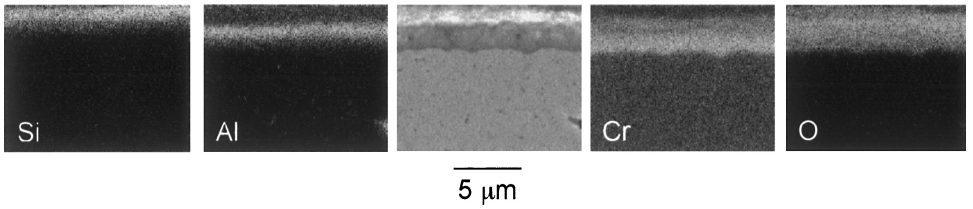

Coated PM1000 after oxidation exposure at 1100°C for 100 h

Fig. 10 Cross-sectional micrographs and elemental x-ray maps of coated superalloys after oxidation.

showed internal precipitation of Al_2O_3. At this time, it is not clear whether coating defects and/or oxygen permeation through the coating contributed to this effect. The coating for Inconel 617 displayed the least oxidation protection, even though the aluminum and silicon maps suggest that the coating was intact. The internal precipitation of Al_2O_3 and the extensive penetration of chromium into the coating suggest that the reaction barrier was not very effective on this alloy.

Oxidation Behavior of Gamma TiAl

The coating concept for protection of gamma TiAl against oxidation is also based on a two-layer coating concept, namely, an oxygen diffusion barrier and a reaction barrier. A silica-based glass layer was used as the oxidation barrier, but for the reaction barrier, two types of layers were evaluated: 1) a $TiAl_3$ layer and 2) an Al_2O_3 layer deposited by the sol-gel process.

Figure 11 summarizes the weight-gain data for both coated and uncoated specimens exposed in air at 870°C. It is evident from Fig. 11 that the coatings were effective in protecting the alloy from oxidation. The best protection was offered when $TiAl_3$ was used as the reaction barrier, but the sol-gel deposited Al_2O_3 worked nearly as well.

Emittance

Although the sol-gel coatings have demonstrated good oxidation resistance on a variety of materials, the emittance of these coatings has been relatively low. Therefore, to optimize the performance of the coating system for both oxidation resistance and emittance enhancement, the multilayered coating concept was again used. Inconel 617 coupons were used as the test material to develop and test the coating concept. Several formulations were applied to Inconel 617 coupons as an outer layer over the oxidation layer, and emittance was determined based on total reflection measurements

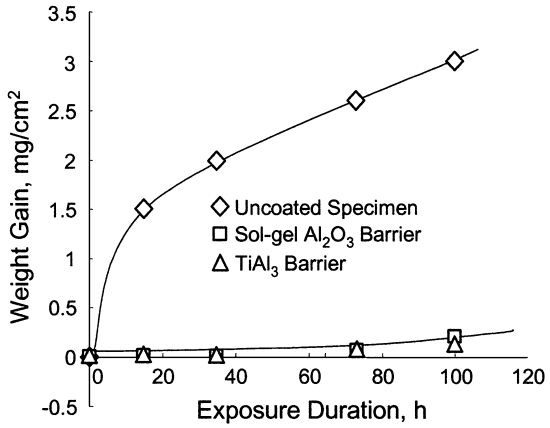

Fig. 11 Oxidation behavior of uncoated and coated gamma TiAl.

at room temperature. The best performance in the as-coated condition was noted with a coating consisting of SiB_6 particles embedded in the sol-gel oxidation barrier coating. To verify the stability of these coatings at high temperatures, the coated specimens were exposed in air at 1000°C. Figure 12 summarizes the results, showing that these coatings exhibited high emittance values, initially approaching 0.9, but that the emittance decreased with increasing exposure. The weight-change data, however, show that the coating was eroded by the exposures and did not remain stable on the surface after longer times. The retention of emittance at a fairly high value suggests that the coating was not lost entirely over the exposure period investigated. On the other hand, the oxidation coating (by itself) retained the original emittance value, albeit low, with a corresponding low weight change.

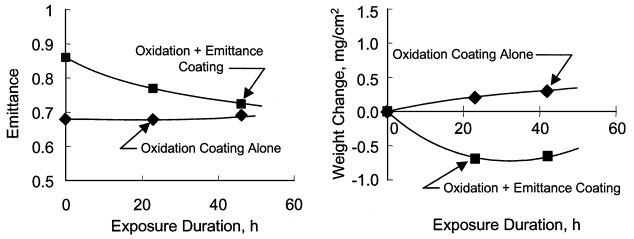

Emittance **Weight change**

Fig. 12 Emittance and weight-change as a function of exposure in air at 1000°C for coated Inconel 617 with emittance coating on top of oxidation coating.

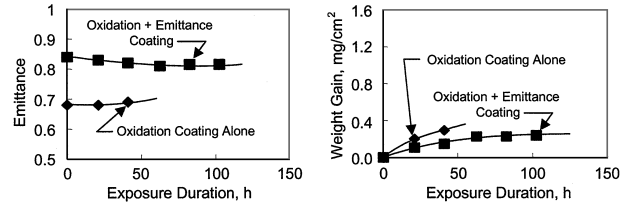

Emittance **Weight change**

Fig. 13 Emittance and weight-change as a function of exposure in air at 1000°C for coated Inconel 617 with emittance coating embedded within the oxidation coating.

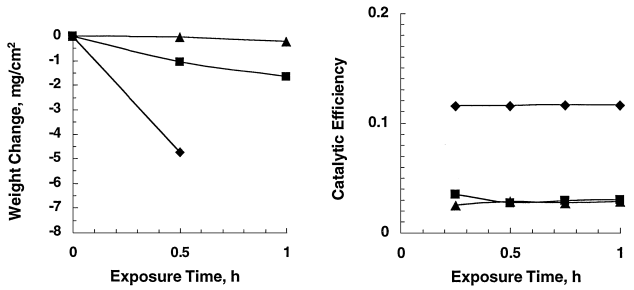

Fig. 14 Oxidation behavior and catalytic efficiency of coated and uncoated Inconel 617 sheet exposed in hypersonic flowing air at 980°C: ♦, uncoated; ▲, sol-gel coating; and ■, Pyromark 2500.

Because the emittance layer was eroding from the coating system during oxidation exposures, an alternate approach was selected in which the emittance layer was embedded between layers of the oxidation barrier coating. Evaluation of the concept was again performed on Inconel 617 alloy, and the results shown in Fig. 13 indicate that the coating remained intact. The weight gain was relatively low, and the emittance values remained above 0.8 throughout the 100-h exposure. In fact, the oxidation performance of the specimen with the emittance layer was even better than that for the specimen coated with the oxidation-resistant layers alone. This improved performance was due to the lower oxygen permeability caused by the greater thickness of the coating with the emittance layer.

Flowing Air Tests

The performance of candidate coatings for Inconel 617 was evaluated in hot flowing air in the HYMETS at 980°C for 1 h, and the results are shown in Fig. 14. Coatings evaluated included LaRC-produced sol-gel coatings, a commercially available high-emittance coating (Pyromark 2500), and uncoated Inconel 617 for reference. For the purposes of evaluating catalytic efficiency of the LaRC-produced sol-gel coatings, the reaction barrier layer and the oxidation-resistant and low-catalysis layers were used, with the low-catalysis layer being the outermost. No emittance layer was included. Specimens were weighed before exposure, after 0.5 h, and after 1 h. The uncoated material was found to lose over 4.5 mg/cm^2 after only 0.5 h of exposure and suffered severe spalling of the oxide layer. The commercial coating suffered a larger amount of weight loss compared to the uncoated material, losing approximately 2 mg/cm^2 after 1 h. The sol-gel-coated sample had the best performance, losing roughly 0.2 mg/cm^2 after 1 h of exposure.

The catalytic efficiency of the Inconel 617 and the sol-gel and the commercial coating as measured in the HYMETS facility is also shown in Fig. 14. Both coatings showed good performance relative to the uncoated alloy, displaying a recombination efficiency of less than 0.03, even after exposure.

Summary

Ultrathin lightweight sol-gel coatings were developed for environmental protection and thermal control for three nickel-based superalloys (Inconel 617, 602CA, and PM1000) and one gamma TiAl alloy that are candidates for hot-structure applications. Tensile tests of uncoated thin-gauge Inconel 617 and 602CA sheets after exposure in air at 980°C for up to 100 h indicated a significant loss of ductility due to oxidation. Microstructural examination revealed a significant amount of oxidation damage to the unprotected alloy sheets. The coatings developed for 602CA, PM1000, and gamma TiAl provided protection against oxidation damage for the alloys. Oxidation weight gain was greatly reduced, and the microstructures of the coated alloys showed that the alloys had not reacted with the environment. The coating developed for Inconel 617 also produced greatly reduced weight gains, but microstructural analysis showed that the alloy reacted with the base layer of the coating, reducing its protective capability. Base layer modifications are being investigated to prevent this interaction with the alloy.

The thermal control attributes of the coatings were also demonstrated using Inconel 617 as a substrate. The emittance layer of the coating imparted an emittance in excess of 0.8 during exposure at 980°C for up to 100 h, which was at least 15% greater than that for the coated alloy without the emittance layer. Likewise, the low-catalysis outer layer of the coating reduced the catalytic efficiency for recombination of atomic oxygen and nitrogen in hypersonic flowing air. The catalytic efficiency of coated Inconel 617 was reduced by a factor of four, compared to the uncoated condition, for a 1-h exposure at 980°C.

Acknowledgments

The authors acknowledge the efforts of B. D. Prasad of Analytical Services and Materials, Inc., and J. M. Baughman of Lockheed Martin Space Operations. B. D. Prasad made significant contributions in the development and application of coatings. J. M. Baughman conducted large numbers of detailed microstructural analyses that led to a greater understanding of oxidation and coating behavior.

References

[1]Brown, W. F., Mindlin, H., and Ho, C. Y. (eds.), *Aerospace Structural Metals Handbook*, Vol. 5, Code 4215, Center for Information and Numerical Data Analysis and Synthesis/U.S. Air Force Cooperative Research and Development Agreement Handbook Operation, Purdue Univ. Press, West Lafayette, IN, 1996.

[2]Krupp VDM, Material Data Sheet 4037, 1996.

[3]"Dispersion Strengthened High-Temperature Materials," Plansee, Bulletin 706 DE 1.98 (3000)RWF, 1998.

[4]Clemens, H., Glatz, W., Eberhardt, N., Martinz, H. P., and Knabl, W., "Processing, Properties and Applications of Gamma Titanium Aluminide Sheet and Foil Materials," *Symposium Proceedings on High-Temperature Ordered Intermetallics VII*, edited by C. C. Koch, C. T. Liu, N. S. Stoloff, and A. Wanner, Vol. 460, Materials Research Society, Pittsburgh, PA, 1997, pp. 29–43.

[5]Young, S. K., "Overview of Sol-Gel Science and Technology," Army Research Lab., Rept. ARL-TR-2650, Aberdeen Proving Grounds, MD, Jan. 2002.

[6]Brinker, C. J., and Scherer, G. W., *Sol-Gel Science: The Physics and Chemistry of Sol-Gel Processing*, Academic Press, San Diego, CA, 1990.

[7]Wiedemann, K. E., Taylor, P. J., Clark, R. K., and Wallace, T. A., "Thin Coatings for Protecting Titanium Aluminides in High-Temperature Oxidizing Environments," *Environmental Effects on Advanced Materials*, edited by R. H. Jones and R. E. Ricker, Minerals, Metals, and Materials Society, Warrendale, PA, 1991, pp. 107–121.

[8]Wiedemann, K. W., Bird, R. K., Wallace, T. A., and Clark, R. K., "A Sol-Gel Derived Coating for Preventing Environmental Degradation of Titanium Beta-21S and its Effect on Mechanical Properties," *Beta Titanium Alloys in the 1990's*, edited by D. Eylon, R. R. Boyer, and D. A. Koss, Minerals, Metals, and Materials Society, Warrendale, PA, 1993, pp. 93–103.

[9]Prasad, B. D., Sankaran, S. N., Wiedemann, K. E., and Glass, D. E., "A Multilayer Coating for Protection of Titanium Aluminides from Oxidation and Hydrogen Embrittlement," *Structural Intermetallics 1997*, edited by M. V. Nathal, R. Darolia, C. T. Liu, P. L. Martin, D. B. Miracle, R. Wagner, and M. Yamaguchi, Minerals, Metals, and Materials Society, Warrendale, PA, 1997, pp. 295–303.

[10]"Standard Test Methods for Tension Testing of Metallic Materials," *Annual Book of ASTM Standards*, Vol. 03.01, edited by R. F. Allen, N. C. Baldini, P. E. Donofrio, E. L. Gutman, E. Keefe, J. G. Kramer, C. M. Leinweber, V. A. Mayer, P. A. Mcgee, K. A. Peters, S. Sandler, T. J. Sandler, and R. F. Wilhelm, Designation E8-99, American Society for Testing and Materials, West Conshohocken, PA, 1999, pp. 57–77.

[11]Clark, R. K., Cunnington, G. R., and Robinson, J. C., "Vapor-Deposited Emittance-Catalysis Coatings for Superalloys in Heat Shield Applications," *Journal of Thermophysics and Heat Transfer*, Vol. 1, No. 1, 1987, pp. 28–34.

[12]Clark, R. K., Cunnington, G. R., and Wiedemann, K. E., "Determination of the Recombination Efficiency of Thermal Control Coatings for Hypersonic Vehicles," *Journal of Spacecraft and Rockets*, Vol. 32, No. 1, 1995, pp. 89–96.

[13]Christ, H. J., Berchtold, L., and Sockel, H. G., "Oxidation of Ni-Base Alloys in Atmospheres with Widely Varying Oxygen Partial Pressures," *Oxidation of Metals*, Vol. 26, No. 1–2, 1986, pp. 45–76.

[14]Douglass, D. L., "The Oxidation Mechanism of Dilute Ni–Cr Alloys," *Corrosion Science*, Vol. 8, No. 9, 1968, pp. 665–678.

[15]Scott, F. H., "Influence of Alloy Additions on Oxidation," *Materials Science and Technology*, Vol. 5, No. 8, 1989, pp. 734–740.

[16]Giggins, C. S., and Pettit, F. S., "Oxidation of Ni-Cr Alloys Between 800 and 1200°C," *Transactions of Metallurgical Society AIME*, Vol. 245, No. 12, 1969, pp. 2495–2507.

[17]Brill, U., and Agarwal, D. C., "Alloy 602CA: A New High Strength High Temperature Alloy for Service up to 1200°C," National Association of Corrosion Engineers International, Paper 226, 1993.

[18]Birks, N., and Meier, G. H., *Introduction to High Temperature Oxidation of Metals*, Edward Arnold, London, 1983, pp. 93, 94.

[19]Weinbruch, S., Anastassiadis, A., Ortner, H. M., Martinz, H. P., and Wilhartitz, P., "High Temperature Oxidation of Fe- and Ni-Base Oxide Dispersion Strengthened Superalloys PM 2000 and PM 1000," *Proceedings of the 14th International Plansee Seminar'97, Vol. 1: Metallic High Temperature Materials*, edited by G. Kneringer, P. Rodhammer, and P. Wilhartitz, Plansee AG, Tyrol, Austria, 1997, pp. 857–868.

S. A. Bouslog
Associate Editor